Development of Micro-Vacuum Arc Thruster with Extended Lifetime

IEPC-2009-192

Presented at the 31st International Electric Propulsion Conference,
University of Michigan • Ann Arbor, Michigan • USA
September 20 – 24, 2009

TaiSen Zhuang, Alexey Shashurin, Lubos Brieda and Michael Keidar

Mechanical & Aerospace Engineering, The George Washington University
Washington DC 20052

Abstract: This paper presents a new configuration of vacuum arc thruster with an aim to extend operational lifetime. Rotation of the cathode spot as a result of an applied magnetic field is demonstrated leading to uniform plasma generation and the possibility of long duration operation. It is shown that a magnetic field leads to an increase in the thruster output by a factor of fifty. Kinetic simulations of the thruster are performed. Simulated results are in good agreement with experimental observation.

I. Introduction

The development of micro-Vacuum Arc Thrusters (VAT) has led to recognition of its advantages for the control of nanosatellites[1]. The design of the VAT is affected by the requirements of the propulsion system, power, mass and complexity. In earlier designs, a bulky high voltage capacitor in the Power Processing Unit (PPU) was used. However, recently, inductive energy storage (IES) was applied in the PPU and this significantly improved the efficiency and reduced the mass of the propulsion system, which is critical for micro- and nanosatellites[2]. A new class of device is known as a magnetically enhanced vacuum arc thruster (MVAT), which is adapting the technology of VAT and adding an external axial magnetic field. It demonstrated a higher thrust to power ratio compared with the conventional VAT[3]. The magnetic field coil placed around the anode of the thruster reduced the width of the plasma plume and therefore reduced the possible contamination of satellite sensors. This paper describes the new configuration of vacuum arc thruster belonging to the MVAT family designed by adapting the advantages of VAT[4]. In order to provide efficient plasma transport, obtain highly directional plume and to preserve high ion velocity contained in cathodic spot we propose to use a curved magnetic field. Special assembly of 12 single probes was used to measure the temporal evolution of the ion current distribution outside the thruster channel. This paper also describes the initial numerical analysis of the thruster. The primary goal of this exercise was to demonstrate the feasibility of the numerical approach. Based on the results, we demonstrate that the proposed new configuration of MVAT is a good candidate for micro-propulsion. Potential applications of the vacuum arc thruster will be discussed.

II. Experimental set up and diagnostics

The MVAT design is schematically shown in Figure 1. Two coaxial titanium arc electrodes are separated by a single insulating ring. Electrodes and isolator rings had outer diameter of 6.35 mm. Anode and isolator ring lengths were about 5 and 1 mm respectively. The insulator is coated with a carbon paint (colloidal graphite in isopropanol) having resistance of the order of 1-10 KΩ (before the arcing). At these conditions breakdown occurs at about 100 V. More detailed information can be found elsewhere[5,6].

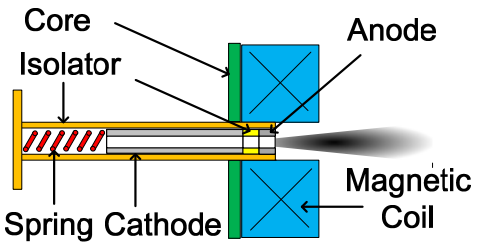

Figure 1: Schematic of the Magnetically Enhanced Vacuum Arc Thruster

A PPU similar to that used previously in Ref. 2, was employed in the current work. The PPU operates in two steps (see Figure 2). On the first step, when the switch (IGBT transistor was used) is open, the inductor used in the circuit is charged by the DC power supply (20-30 V). On the second step, energy accumulated in the inductor is applied to arc electrodes (when the switch is closing). This results in a peak voltage of LdI/dt (up to several hundred volts) between electrodes and causes the breakdown. Breakdown forms at the isolator ring surface covered with conductive carbon coating which separates titanium arc electrodes. These micro-plasmas generated at the isolator ring interface triggers the arc between the arc electrodes. The current flowing in the inductor is fully switched to the vacuum arc load after IGBT switch opening. Typical arc currents were 35-40 A and the basic design of the inductive energy storage circuit is shown in Figure 2.

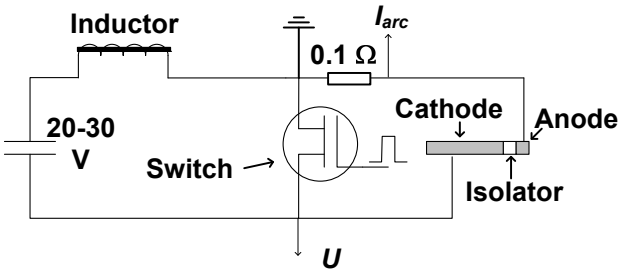

Figure 2: Equivalent circuit of an Inductive Energy Storage (IES) PPU for the VAT

The magnetic coil (with attached to it 1020 steel core) is mounted coaxially to the electrodes and used to produce the curved magnetic field in the thruster channel (see Figure 1). The magnetic coil with core is movable in axial direction in order to provide certain strength and configuration of magnetic field. A typical configuration of the magnetic field is shown in Figure 3 for coil current I_{coil}=20 A. The system uses a coil of 0.5 mm diameter copper wire with 700 turns. It is co-axial with the electrode axis and a magnetic core (steel 1020) has the shape of a washer with a thickness of about 2 mm, see Figure 1.

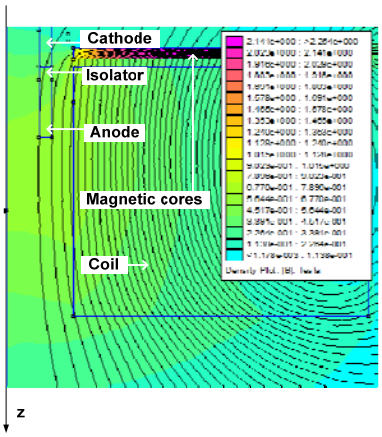

Figure 3: Simulation of the magnetic field applied to thruster for coil current of 20A.

The magnetic field has two main purposes. First, this configuration of the magnetic field keeps the arc spots at the boundary between the metallic cathode and insulator[7]. Multiple spots exist with a current per spot of about 10-30 A depending on the cathode material. In addition, the magnetic field leads to cathode spot motion in the azimuthal direction, well-known as –JxB[7], thus causing uniform erosion of the cathode from the side facing the insulator. The spring pushes the cathode to the insulator providing a long life-time and stable operation of the thruster. The metallic film deposited onto the insulator surface evaporates during the arc spot formation providing smooth conditions for forming the arc spot[6]. The second purpose of the magnetic field is to transform radial cathodic jet flow into axial flow. An overall schematic of the thruster and plume is shown in Figure 4. Previous calculations using the hydrodynamic approach show that in such a magnetic field configuration, the radial cathodic jet flow may be effectively transformed into axial flow allowing the plasma to be confined inside the thruster channel and thus reducing losses to the walls[3]. A typical calculated plasma density distribution inside the thruster is shown in Figure 4.

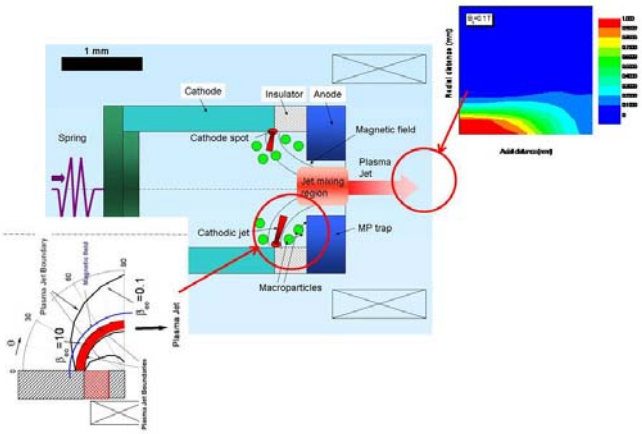

Figure 4: Schematics of the micro-cathodic arc thruster. Inset (lower-left side) shows the calculated plasma jet geometry during the transport in the curved magnetic field guide. Inset (right side) illustrates a normalized plasma density distribution in the vacuum arc plasma jet that determines the plasma plume profile.

4-probe assembly was used to measure the rotation velocity of the cathode spot. Four single probes were located along the azimuth inside the thruster channel as shown in Figure 6 . Probes were covered with insulating heat shrink tubes along their whole length except small part (about 1 mm) facing the cathode-isolator interface. Probes were biased about -30 V with respect to grounded cathode.

Total ion current in the output thruster jet was collected to the negatively biased chamber walls (-40 V with respect to the grounded cathode) and measured from 50 Ω shunt resistor. Arc current was measured from 0.1 Ω shunt resistor.

III. Experimental Results

Figure 5 shows the waveforms of voltage between arc electrodes U and current in inductor I_{ind}. Energy is accumulated in inductor from -1.5 ms to 0 and I_{ind} reached about 40 A prior the breakdown. Breakdown occurs at t=0 by closing the IGBT switch (see Figure 2) which causes voltage peak applied to arc electrodes observed at t=0. Note, for t<0 (when switch is open) I_{ind} is equal to current flowing through the switch, while for t>0 I_{ind}=I_{arc} and U=U_{arc}, where I_{arc} and U_{arc} are arc current and arc voltage respectively. Typical arc voltage was about 50 V, arc current decreased from 35-40 A to 0 and arc duration was several hundred microseconds.

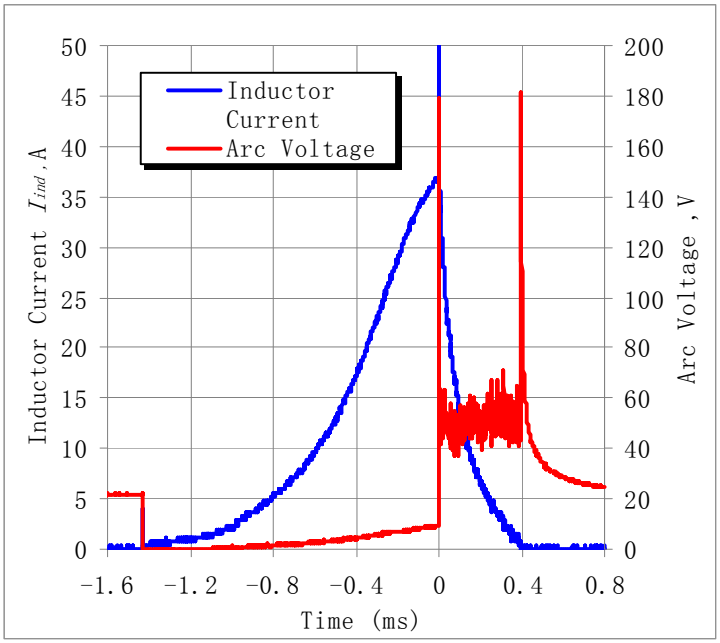

Figure 5: Temporal evolution of voltage between anode and cathode, and inductor current.

Typical signals obtained from the 4-probe assembly are presented in Figure 6. It was observed that arc was rotated in -JxB direction and rotation velocity slightly decreased with arcing time. An average velocity was about 75 m/s. It is seen from Figure 6 that spot complete full revolution around the inside cathode surface, which is critical for homogeneous cathode erosion and thruster lifetime.

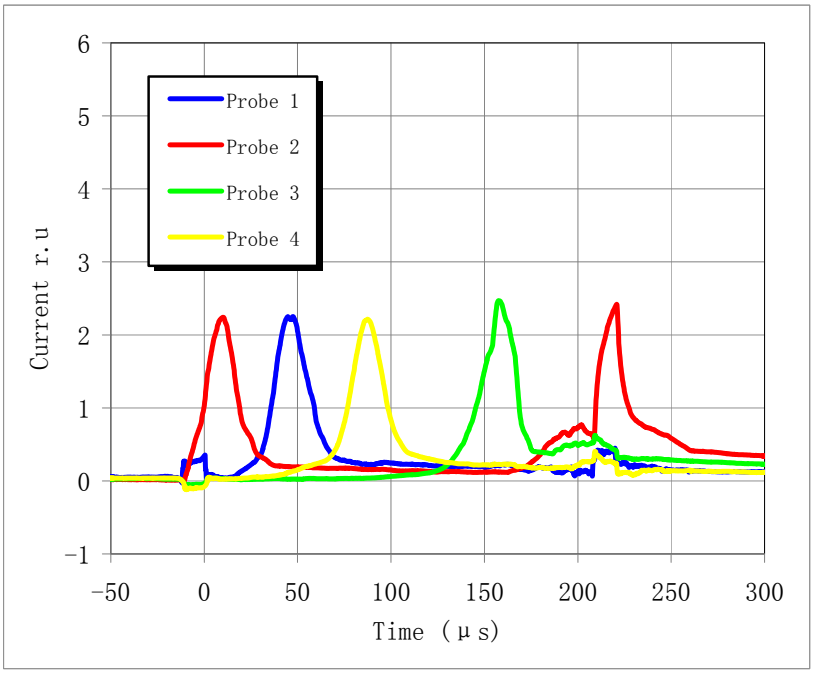

Figure 6: Temporal evolution of signals from 4-probe assembly indicating rotation of cathodic spot rotation

Figure 7 and Figure 8 indicates the effect of magnetic field on thruster output. Figure 7 shows photographs of the plasma plume without (on the left) and with (on the right) the magnetic field applied. It is seen that strong plasma plume having the length of about 7cm was observed with magnetic field applied in contrast with almost no

jet without magnetic field. Figure 8 presents the temporal evolution of output jet current I_{jet} for different currents in coil. It is seen that applying the magnetic field results in very significant increase of I_{jet}.

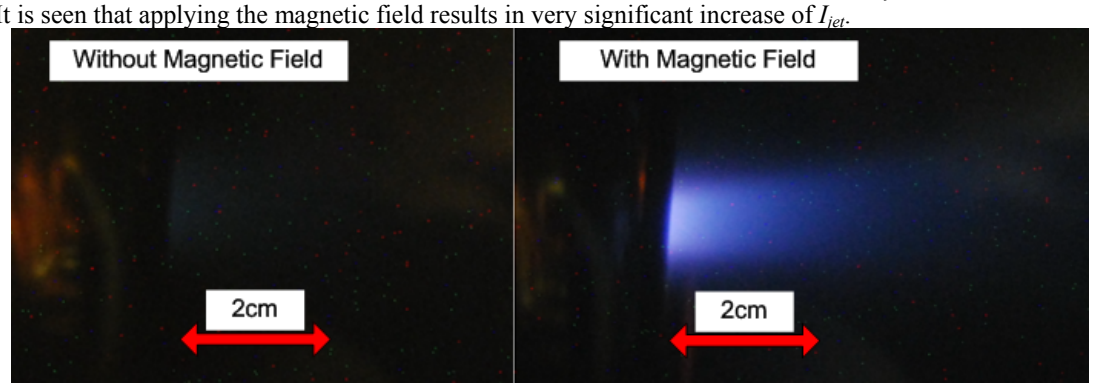

Figure 7: Two photographs of the plasma plume without and with the magnetic field applied

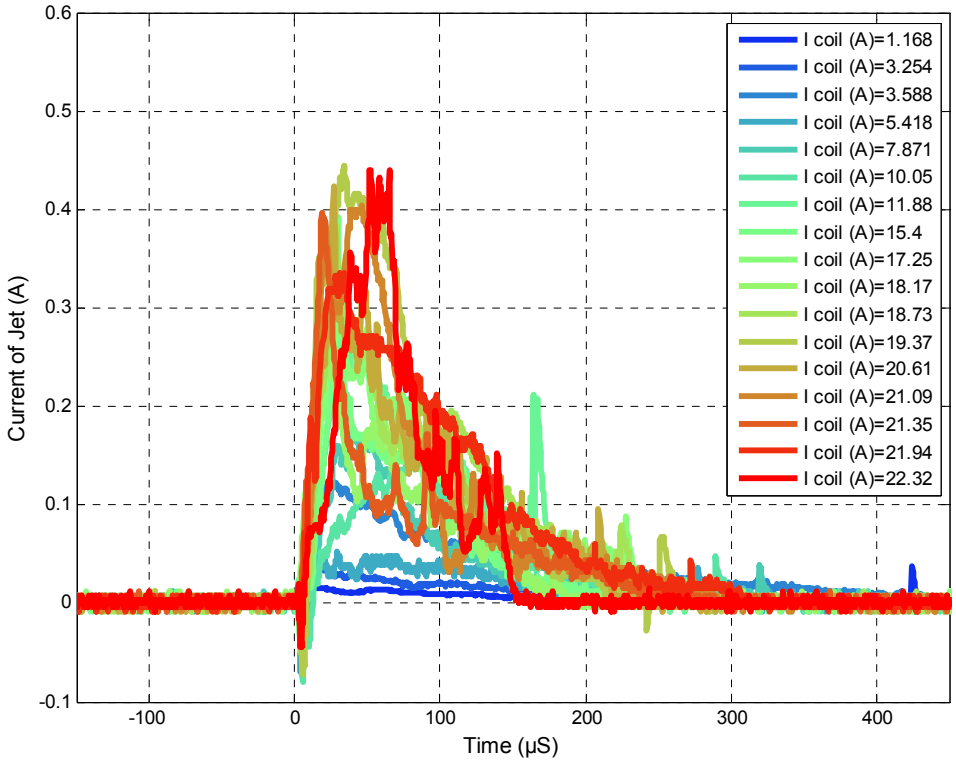

Figure 8: Time-Jet Current distribution with different magnetic field coil currents

Figure 9 shows the dependence of ratio $f = \frac{I_{jet}}{I_{arc}} \times 100\%$ on the coil current I_{coil}. It was observed that without magnetic field the thruster output was low: f=0.06%. Increase of the magnetic field resulted in significant output increase (up to 50 times), which finally saturated at f~3-3.5%. Note, that f cannot exceed the $f_{\max} = \frac{I_{\max}}{I_{arc}} \times 100\%$, where I_{max} is the total jet current generated from the cathodic spot. According to Kimblin[8] the f_{max} for Titanium is about 8%. Thus f ~3-3.5% observed in the experiment corresponds to the efficiency of cathodic jet transport through the thruster channel of about 45%.

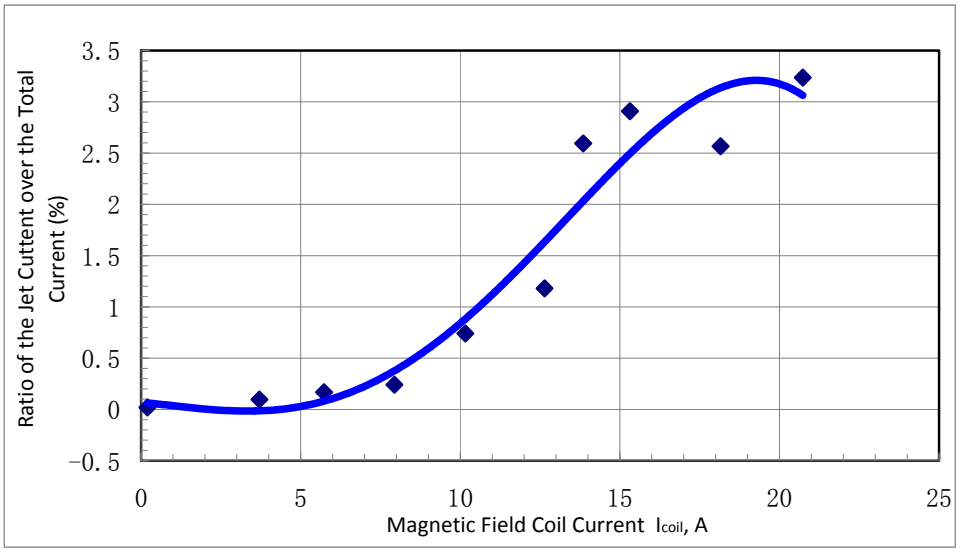

Figure 9: Experiment results of the change of ratio of the jet current over the total arc current with change of magnetic field coil current. The angle between the magnetic field line and the thruster axis at the cathode-isolator interface was 4.6°

Distribution of ion current outside of the thruster channel was measured by the assembly of 12 probes as shown in Figure 10. 12 probes separated 1 cm from each other were installed on the adjustable holder as shown in Figure 10.

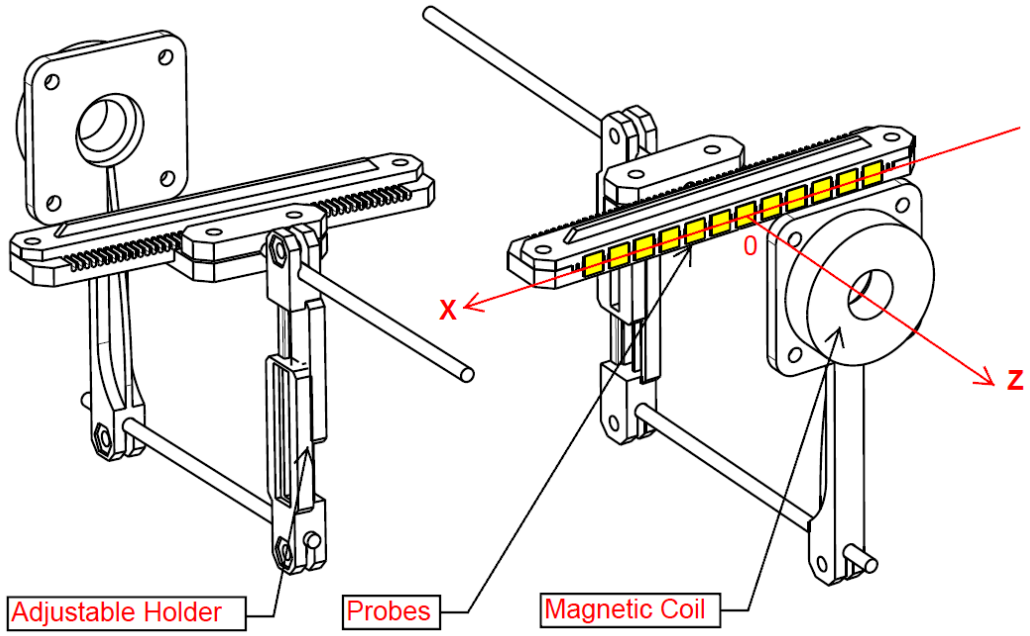

Figure 10: Assembly of 12 probes used to measure the distribution of ion current outside of thruster channel.

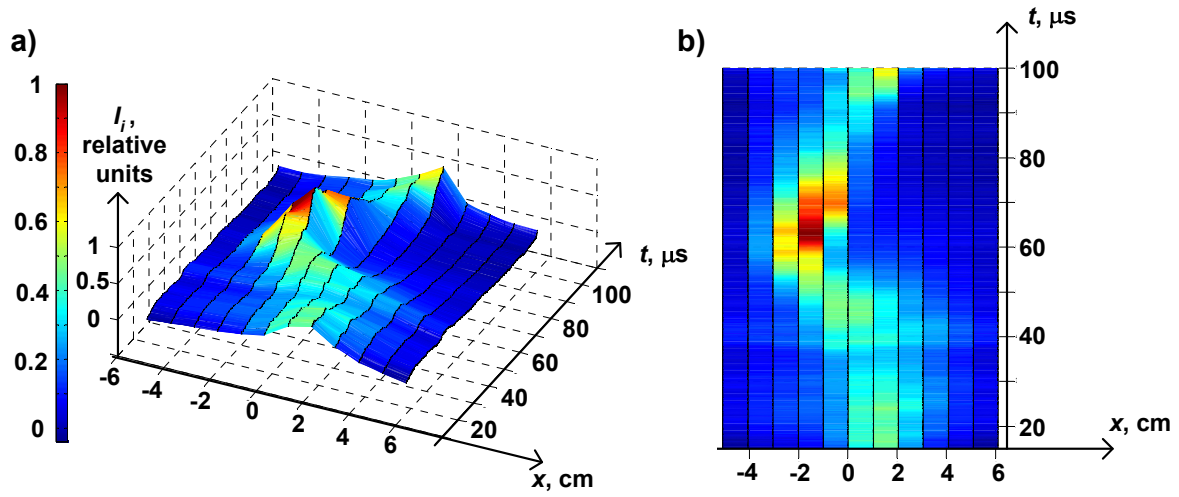

Figure 11: Temporal evolution of ion current (I_i) radial distribution measured at 7.6 cm from the thruster exit

Figure 11 shows the distributions of ion current at different moments of time during a single pulse. Let us first consider t=20 μs after arc initiation. It is seen that ion current peak is shifted about 1.5 cm from the thruster axis. Simulations of the thruster coil magnetic field indicates that a magnetic field line passing through this point (x=1.5 cm, z=7.6 cm) is originated from the cathode-isolator edge (see Figs.1,2). This indicates that plasma produced in the cathode spot at the cathode-isolator edge is guided along the magnetic field line. Now let us consider the temporal evolution of ion current peak shown in Fig.11. It is seen that the ion current peak appears first at x= 1.5 cm (at t=20 μs), then shifts to x= - 1.5 cm (at t=65 μs) and finally returns back to x=1.5 cm at t=100 μs. This clearly indicates that plasma jet, guided along the magnetic field, is rotating. Plasma jet rotation follows the rotation of cathode spot which is presented in Figure 6.

IV. Plasma simulations

We also completed initial numerical analysis of the thruster. The primary goal of this exercise was to demonstrate the feasibility of the numerical approach. We were interested in determining whether a fully-kinetic approach, in which both electrons and ions are treated as particles, is suitable for modeling the turning of the ion beam, and the increased ion velocity observed experimentally. As such, we set up the simulation using the 3D electro-static particle-in-cell code Draco. This code was initially developed to study the interaction of electric thruster plumes, but has since been applied to a wide array of applications, including spacecraft charging, ion optics modeling and thruster neutralization studies. [9,10,11,12]

In our work, we considered two cases. The first case did not contain any magnetic field. In the second case, the background magnetic field was loaded, corresponding to coil current of 20A. In this configuration, the magnetic field lines form an angle of approximately 15 degrees from the cathode surface at the location of the cathode spot. Since Draco is a 3D code, we represented the axi-symmetric geometry (to reduce computational overhead) by modeling a thin slab, in which the periodic boundary condition was applied to the front and the back face. The simulation domain can be seen in Figure 12. Cathode is shown by the orange rectangle. The gray rectangle is the insulator, and the blue shape is the anode. Potential difference of 50V was applied between the electrodes. Electrons and ions were injected from a small control surface located at the junction of the cathode and the insulator at flow rates corresponding to 0.4A. We assumed that the beam consisted solely of electrons and doubly charged Ti^{2+} ions. Neutral particles were not modeled directly, but instead we loaded a constant background density corresponding to 6×10^{-5} Torr. Collisions were included through the MCC scheme with cross-sections determined from analytical models. Momentum transfer and Coulomb collisions were considered. The simulation contained 10x50x226 cells, and approximately 2 million particles. No artificial scaling of permittivity was performed.

Figures 12-15 show the preliminary results. Comparison of Figures 12 and 13 clearly illustrates the influence of the magnetic field. In Figure 12, in which there is no magnetic field, the ions are seen to simply diffuse out uniformly in both axial directions. A very small thrust is expected to be generated in this configuration. However,

the addition of the magnetic field, Figure 13, clearly shows the extraction of the ion beam from the thruster. It should be pointed out that ion transport along the magnetic field line predicted by simulations is in agreement with ion current measurements as shown in Fig.11. Even more interesting is the effect of the magnetic field on the axial ion velocity. In the absence of the magnetic field, the velocity reaches 16km/s at 1cm away from the anode end. However, as can be seen in Figure 15, addition of the magnetic field results in increase of the velocity to approximately 43km/s. Additional analysis will be performed as future work.

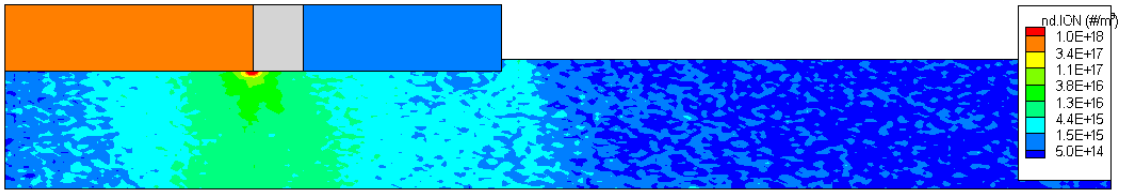

Figure 12. Ion density, no magnetic field

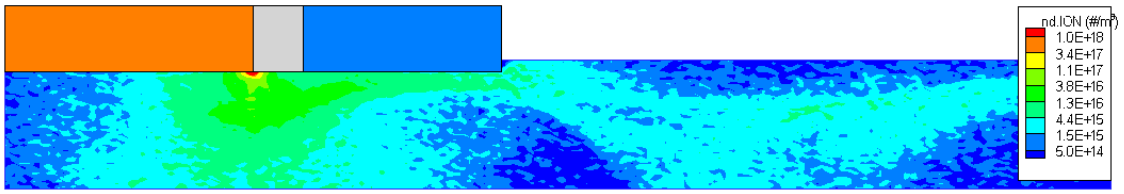

Figure 13. Ion density, magnetic field

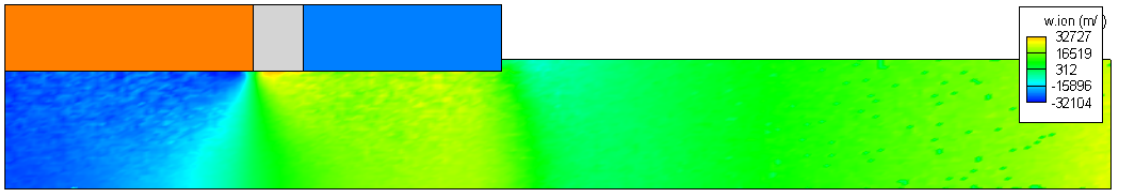

Figure 14. Axial ion velocity, no magnetic field

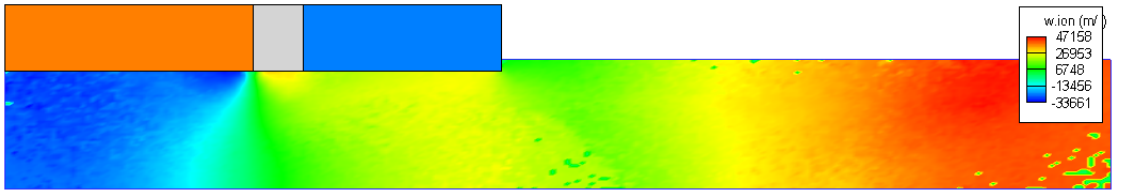

Figure 15. Axial ion velocity, magnetic field

V. Conclusion

It was demonstrated that an applied magnetic field leads to several interesting effects. A magnetic field results in arc rotation which, in turn, leads to homogenous erosion critical for thruster long time performance. It was shown that output ion current increases by a factor of fifty with an applied magnetic field. Kinetic simulations qualitatively explain the observed effect of the magnetic field on plasma transport along the magnetic field.

References

[1] M. Keidar, J. Schein, K. Wilson, A. Gerhan, M. Au, B. Tang, L. Idzkowski, M. Krishnan, I. I. Beilis, Magnetically enhanced vacuum arc thruster, Plasma Source Science & Technology , 14, 2005, pp. 661-669.
[2] J. Schein, N. Qi, R. Binder, M. Krishnan, J. K. Ziemer and J. E. Polk, A. Anders, Rev. Sci. Instrum., 73, 925

(2002).
[3] M. Keidar and J. Schein, Proceedings of 40th Joint Propulsion Conference and Exhibit, 11 – 14, July 2004 Fort Lauderdale, FL (American institute of Aeronautics and Astronautics, Reston, VA, 2004), AIAA- 2004-4117
[4] Schein, J., Krishnan, M., Ziemer, J., Polk, J "Adding a "Throttle" to a Clustered Vacuum Arc Thruster" AIAA paper 2002-5716, Nanotech, 2002.
[5] A. Anders, I. G. Brown, R. A. MacGill, and M. R. Dickinson, J. Phys. D 31, 584 (1998).
[6] A. Anders, J. Schein, and N. Qi, Rev. Sci. Instrum. 71, 827 (2000)
[7] Vacuum Arc Science and Technology, edited by R.L. Boxman, P.J. Martin and D. M. Sanders (Noyes, New York, 1995).
[8] C.W. Kimblin J. Appl. Phys., 45, 5235 (1974).
[9] Brieda, L., Pierru, J., Kafafy, R., and J. Wang, "Development of the Draco Code for Modeling Electric Propulsion Plume Interactions", 40th Joint Propulsion Conference, Fort Lauderdale, FL, 2004, AIAA-2004-3633.
[10] Brieda, L. and J. Wang, "Modeling Ion Thruster Beam Neutralization", 41st Joint Propulsion Conference, Tucson, AZ, 2005, AIAA-2005-4045
[11] Barrie, A., Spicer, R., and J. Wang, "Modeling Surface Charging with Draco Electric Propulsion Simulation Package", 42nd Joint Propulsion Conference, Sacramento, CA, 2006, AIAA-2006-5022
[12] Nakles, M., Brieda, L., Reed, G., Hargus, W. and R. Spicer, "Experimental and Numerical Examination of the BHT-200 Hall Thruster Plume", 43rd Joint Propulsion Conference, Cincinnati, OH, 2007, AIAA-2007-5305